Received: 7 October 2021 | Revised: 20 December 2021 | Accepted: 23 December 2021

DOI: 10.1111/ijac.14004

International Journal of Applied Ceramic Technology

SPECIAL ISSUE ARTICLE

Bio-derived sodium silicate for the manufacture of alkali-activated binders: Use of bamboo leaf ash as silicate source

Raffaele Vinai | **Fabrice Ntimugura** | **Will Cutbill** | **Robert Evans** | **Yize Zhao**

College of Engineering, Mathematics and Physical Sciences, University of Exeter, Exeter, UK

Correspondence
Raffaele Vinai, College of Engineering, Mathematics and Physical Sciences, University of Exeter, Exeter EX4 4QF, UK.
Email: r.vinai@exeter.ac.uk

Abstract

Alkali activated binders are a promising alternative to the use of Portland cement in the manufacture of concrete for curbing CO_2 emissions. Novel sources of silicates have been investigated in recent years for reducing cost and environmental impacts associated with the use of chemical activators. This study describes the production of solid sodium silicate (SS) activating powder from bamboo leaf ash (BLA). Bamboo leaves were calcined at 550–800°C, mixed with NaOH pellets, and heated in an oven at 300°C. The obtained silicate powder was used for activating blended fly ash/slag samples. Mechanical and microstructural properties of BLA-based samples were compared to those of samples made with commercially available chemicals. The strength of BLA-activated mortars matched the commercially-sourced activators, being 25–30 MPa at 7 days and exceeding 40 MPa at 28 days. The microstructural analysis suggested that BLA-based SS showed a lesser degree of dissolution of precursors at 7 days, but the quality of the matrix was higher than that of NaOH-activated samples. These results confirmed that the reactivity of BLA-silicate powder was similar to that of commercial SS solutions, and show the potential valorization of future biomass renewable waste in the production of low carbon, alkali-activated concretes.

KEYWORDS
cement, geopolymers, microstructure, thermal treatment

1 | INTRODUCTION

Current worldwide concern over the carbon emissions of the construction sector relates mainly to the use of Portland cement in the manufacture of concrete. Due to the limestone calcination and the combustion of fuel for heating the kiln (up to 1450°C), Portland cement production is deemed responsible for about 5%–7% of the world's CO_2 emissions.[1] Alkali activation of aluminosilicate and calcium silicate materials for the production of inorganic binders called alkali-activated materials (AAM – sometimes referred to as 'geopolymers', although this term should preferably be used in relation to low calcium sub-family of AAM) has been extensively investigated in the last decades. AAM can show mechanical and durability properties equal or superior to those of

Portland cement concrete, but with reduced associated carbon emissions.[2,3] Fly ash (FA), metakaolin (MK), and ground granulated blast furnace slag (GGBS) are the most common low calcium (aluminosilicate) and high calcium precursors respectively, used in conjunction with a range of liquid/solid mixes of activators. These activators, typically alkali hydroxide and alkali silicate, provide both a high pH environment (>12) for the dissolution of alumina and silicate species, as well as free silicates to sustain the formation of ortho-silicate ions (SiO_4)[4] in sialate-siloxo chains, that is, the backbone of AAM. However, sodium silicate (SS) used in combination with sodium hydroxide (SH) as a commonly adopted blended alkaline activator for AAM remains expensive and carbon-intensive.[4]

In recent years, research worldwide has been focussing on the development of powders and nano-powders for different applications. Nanopowders used in AAM technology,[44] metallurgy,[45] and glass technology[46] have been successfully obtained even from waste or by-products. Waste-derived silicate activators for AAM have been proposed, demonstrating the suitability of such alternative activators both in terms of mechanical strength development[5–7] and environmental as well as economic benefits.[8–10]

Several sources of waste-derived silicates have been investigated in the literature for their use as activators.[11] Mining waste such as iron ore tailings,[12] glass waste,[7,13] and silica fume[14,15] are among the inorganic Si-rich waste streams successfully utilized for the production of activators for AAM.

Significant availability of Si-rich waste can be found from biomass combustion by-products. The biomass ash (BMA) chemical composition can vary over a wide range of elements according to the nature of the biomass itself (e.g., wood, non-wood, and aquatic) as well as to the properties of soil on which the vegetal species are growth (e.g., plants growth on clayey soil vs. the growth on humus-rich soil). Nonetheless, an average SiO_2 amount of around 45% in ash derived from grasses and straw can be expected, whereas wood biomass shows lower SiO_2 average contents (~22%).[16]

The current shift and advances in biofuels suggest the high availability of BMA. The actual trend in the adoption of biomass in the UK national energy mix indicates that almost 40% of the energy consumption from renewable and waste sources is from biomass, ahead of solar and wind energy. Some of the conventional BMA valorization strategies include its use as cementitious materials, mainly due to the high content of reactive silica. BMA was investigated for partial substitution of Portland cement for their pozzolanic potential.[17–19]

Most of the studies on the incorporation of BMA in geopolymer concrete or alkali-activated composites cover the partial substitution of the traditional precursors (such as FA, GGBS, or MK). The potential use of non-wood BMA in alkali-activated concrete as a source of silica and alkalis, when combined with coal FA and activated with SS and SH to produce binders based on aluminosilicate hydrates, were reported.[20,21] Positive effects including pore-filling effect, formation of less ordered and homogeneous microstructures, and the dual formation of calcium silicate hydrate and highly geo-polymerized units were reported for palm oil fuel ash.[22]

The relatively high silica content of non-wood BMA suggests its potential use in the production of alkali silicate for the activation step. The use of BMA in the production of silicate activators for AAM has not been extensively investigated yet. Significant research has been carried out mainly on the use of rice husk ash (RHA), with most of the available literature proposing hydrothermal dissolution of RHA in alkali (sodium or potassium) hydroxide solutions varying concentration, temperature, and process time.[6,14] Few other BMA materials have been studied to date. Moraes et al. investigated the use of sugar cane straw ash (SCSA) as a silica source for the production of alkaline activating suspensions.[23] The authors used a simple dissolution thermal bottle and various parameters were investigated including dissolution time, and water/NaOH/ash ratios in mixes. Results suggested that SCSA based systems exhibited reaction products similar to those observed in matrices of commercially available SS activated mortars. Extraction of alkali silicates from BMA was also demonstrated by Dodson and colleagues, who worked on a range of BMA, mainly wheat straw[24] and miscanthus bottom ash.[25] They described the opportunities of successfully extracting alkali silicates for various applications, although concrete production was not mentioned among those.

Bamboo is a type of giant woody grass that grows in approximately 3.2% of the world's total forest area, which accounts for 38 billion hectares.[26] It takes around 3–6 years to harvest depending on the species. During the harvest, the rhizome remains intact, thus new culms can grow back without the need for replanting. It is estimated that a bamboo culm can yield about 0.7–0.9 kg of leaves (dry mass) at the harvest time. Assuming an average production of 5000 culms/ha/year, the availability of bamboo leaves (BL) after the harvest of culms is in the range of 4–5 t/ha/year.[27–30] In countries such as India, where 10 million hectares are cultivated with bamboo, the production of leaves can therefore be estimated at 50 million tons each year, which are currently considered waste.[31]

BLA has been investigated as a pozzolanic material for partial Portland cement substitution.[32–35] Kow et al. investigated the hydrothermal extraction of silica from BLA in NaOH solution for the production of water glass, aiming at the development of BLA-based aerogel materials.[36]

Alkali extraction of Si from BLA was also discussed by Olawale et al. targeting the production of Si for solar cell components.[37] To the best of the authors' knowledge, the use of BLA as a silica source for AAM activation has not been described yet in the literature.

In addition to the search for alternative silica sources for activators, the practicalities of handling large amounts of highly corrosive liquid activating solutions have motivated the development of solid-based 'one-part' activators.[38] The development of alternative 'one-part' silicate activators seems to be the next direction for sustainable geopolymer binders for application in mortars and concrete.

The main objective of this study was to assess the potential of using BLA for the production of an alkaline activating powder for the production of alkali-activated mortars. BLA was added to SH pellets and heated to a moderate temperature to allow a thermo-chemical reaction that transformed amorphous BLA in a crystalline SS powder, according to the method proposed by Vinai and Soutsos.[7] The effectiveness of the produced BLA-silicate powder in activating FA/GGBS blends was assessed through a comparison against mortars produced using commercial chemicals and through microstructural analysis on pastes with scanning electron microscope (SEM) images coupled with energy-dispersive X-ray spectroscopy (EDS).

2 | MATERIALS AND EXPERIMENTAL METHODS

2.1 | Materials

Stems from bamboo species *Arundinaria japonica* were locally sourced, chopped down, and stripped off their leaves. Three batches of leaves were harvested in three consecutive years (2019, 2020, and 2021), i.e., over the duration of the investigation, in order to crosscheck the robustness of the results over several harvests, and thus the appropriateness of the proposed valorization strategy in real applications. Leaves were oven-dried at 50–70°C for 48–72 h, see Figure 1. Dried BL were milled into a fine powder and tested with X-ray diffraction (XRD) and thermogravimetric analysis (TGA).

The calcination of BL was carried out at two temperatures: at 550°C for 4 h (batch 1), and at 800°C for 2h (batches 2 and 3). The calcination method was chosen according to the results of TGA on raw BL (see Section 3.1.1. and Figure 3), investigating the effects of the variation of temperature and calcination time on the properties of the BLA. The ash was allowed to cool down at room temperature with natural ventilation. The BLA was subsequently ground using a pestle and mortar to a fine powder that was stored in airtight sealed bags. In order to check the effect of the quality of the milling step, the BLA produced with batch 2 was ground in a ball mill prior to its utilization for the production of the activator. Experiments with ash from batch 1 (BLA-1) were primarily focused on the determination of the strength development over time, from 1 to 28 days of age. Experiments with BLA-2 were aimed at assessing the chemical nature of the leaves and the effect of water content on strength development. BLA-3 was mainly produced for the microstructural investigation of paste. Mortar mixes tested at 7 days of curing were manufactured using BLA-2 and BLA-3 (and equivalent commercially available chemicals) for an overall assessment of the effect of a range of parameters (water content, temperature of calcination of leaves) and for checking the consistency of the quality of the BLA-based activator.

FA and GGBS were used as precursors. FA was obtained from a coal-fired power plant in the UK (Drax Power plant) and GGBS was sourced from Ecocem, Ireland. Particle densities were 2.42 and 2.92 g/cm^3 for FA and GGBS respectively. Oxide compositions from X-ray fluorescence (XRF) analysis for FA and GGBS are shown in Table 1. The benchmark, commercially available chemical activator was a mixture of SS (12.8% wt.% Na_2O, 25.5 wt.% SiO_2, and 61.7 wt.% water) sourced from Fisher Scientific, and 30% wt. NaOH solution obtained from NaOH solid pellets dissolved in water. For the production of mortar, silica sand with grain distribution <4 mm was used.

2.2 | Preparation of BLA activator powder and alkali-activated mortars

The production of solid SS activator from BLA was achieved in three steps, following the method proposed by Vinai and Soutsos[7]: (a) the amount of SiO_2 from BLA was assessed either interpreting results from SEM/EDX (batches 1 and 3) or XRF (batch 2), (b) the amount of NaOH powder required was calculated considering a molar ratio equal to 1 in $Na_2O + SiO_2 \rightarrow Na_2SiO_3$ and considering that Na_2O content in NaOH powder is 77.5%, and (c) BLA and NaOH powders were mixed with small amount water to reach a homogeneous paste-like consistency and then heated to 300–330°C for 1h. The obtained hardened paste was subsequently crushed down for its use in producing AAM mortars.

A FA/GGBS blend with a mass ratio of 60%/40% was used as a binder precursor. Silica sand proportioned with sand:binder ratio of 2.75 was added to the mixes. Activation parameters alkali dosage (M+), that is, the mass ratio Na_2O/dry precursor blend, and alkali modulus (AM), that is, the mass ratio Na_2O/SiO_2, were chosen equal to 7.5% and 1%, respectively, for the mixes with BLA-based activator as well as with commercially available solutions.

FIGURE 1 (Left) Harvested leaves. (Centre) Oven-drying step. (Right) Dried leaves

TABLE 1 Oxide composition (%w) of fly ash (FA) and ground granulated blast furnace slag (GGBS)

Oxide	SiO_2	Al_2O_3	Fe_2O_3	MgO	CaO	Na_2O	K_2O	P_2O_5	Mn_2O_3	SO_3	Others (minor)	LOI
FA	50.2	21.8	10.2	1.8	4.3	0.7	2.7	0.3	0.1	0.1	1	6.4
GGBS	34.9	11.2	0.4	7.9	41.3	0.3	0.3	0.0	0.2	1.8	0.9	0.9

Abbreviation: LOI, loss on ignition.

TABLE 2 Mix proportions of produced mortars. BLAA: Bamboo leaves ash-based activator, SS: Commercial sodium silicate solution, SH: Commercial sodium hydroxide solution. Quantities in g

Mix	FA	GGBS	Sand	SS	SH	BLAA	Water
1-BLAA-0.49	300	200	1375	–	–	130	282
1-SSSH-0.49	300	200	1375	147	80	–	135
1-SH-0.49	300	200	1375	–	161	–	151
2-BLAA-0.43	300	200	1375	–	–	107	247
2-SSSH-0.43	300	200	1375	147	80	–	100
2-SH-0.43	300	200	1375	–	161	–	118
3-BLAA-0.40	300	200	1375	–	–	97	230
3-SSSH-0.40	300	200	1375	147	80	–	83
3-SH-0.40	300	200	1375	–	161	–	102

Abbreviations: FA, fly ash; GGBS, ground granulated blast furnace slag.

A mix with AM = ∞ (i.e., no SiO_2) was also prepared using NaOH solution as the only chemical in order to provide a benchmark for the absence of silicate in the activator. The amount of BLA-based activating powder was calculated according to its assumed chemical composition, which was estimated from the quantity of SiO_2 identified in the three ash batches. Table 2 shows the mix proportioning details of the mortar samples, cast in 50-mm cubic PVC molds. Mixes were labeled after the following sequence: batch – activator – w/s ratio. The quantities were designed for a volume slightly in excess of 1 L of mortar per mix.

Paste samples were produced for the characterization of the microstructure of the binding matrix using BLA from batch 3 and a w/s ratio equal to 0.335. The small quantities required for the paste production were mixed manually in a container and then transferred to cuboid molds (about 20 mm size) for subsequent SEM/EDS analysis. Proportions for pastes are shown in Table 3.

TABLE 3 Mix proportions of pastes. Bamboo leaf ash (BLA)-based sodium silicate (BLAA), sodium silicate (SS), sodium hydroxide (SH) as in Table 2. Quantities in g

Mix	FA	GGBS	SS	SH	BLAA	Water
3-BLAA-0.335P	30	20	–	–	9.7	19.3
3-SSSH-0.335P	30	20	14.7	8	–	4.6
3-SH-0.335P	30	20	–	16.1	–	6.7

Abbreviations: FA, fly ash; GGBS, ground granulated blast furnace slag.

2.3 | Characterization methods

The XRD of powders was carried out on the Bruker D8 Advance diffractometer with a Cu Kα of a wavelength 1.5418 A. The generator was calibrated to a voltage of 40 kV and a current of 40 mA and a goniometer speed of 0.017–0.031° 2θ/s over the range 5–80° 2θ. Each spectrum was processed with "Match!" software containing the crystallographic information files from the crystallography open database (COD.cif files). The chemical composition of raw materials (FA, GGBS, and BLA) was determined by XRF using a Bruker-AXS S4 Pioneer XRF Spectrometer (WDS XRF). The chemical composition of ash from batch 2 was assessed through the XRF method on approximately 6 g of ash dried at 105°C for 1 h. The ash was then placed into a pre-ignited, pre-weighed platinum crucible and ignited at 1000°C for 1 h to determine the mass of volatiles such as CO_2 still left in the sample (loss on ignition, LOI). The sample melted and bubbled, forming a single lump, which had to be crushed using a pestle and mortar for the next preparation stage. As result of the unusual behavior of the sample, another LOI test was performed at 700°C. In contrast, this specimen remained a powder, and both the materials (i.e., BLA ignited at 1000°C and 700°C) were prepared as a fused bead. This was done via a Phoenix fusion machine, which fused 1.5 g of the ash with 7.5 g of lithium borate flux and cast them into a platinum dish to form a glass bead. TGA was performed with a Mettler Toledo TGA/DSC1 STARe system on a temperature range of 25–800°C. The microstructure of ash and raw materials was observed under Tescan Vega 3 SEM coupled with Oxford Instrument X-MAXN EDS detector. The electron beam was set at 20.0 kV, the emission at 22 μA, and the 1.10–10 mbar low vacuum was used for all samples. Compressive strength was assessed with an MCC8 multi-test hydraulic system under load/stress control with a pre-load of ~10 kN and a loading rate of 0.4–0.8 MPa/s. Due to the limited availability of ash and the number of parameters to be checked, a compromise on the total number of samples to be tested were required. Two samples at each age were tested in batches 1 and 2 test series, whereas three mortar cubes were tested for batch 3 test series.

3 | RESULTS AND DISCUSSION

3.1 | Chemical composition and microstructure of BL and BLA

3.1.1 | Bamboo leaves

XRD diffractogram of powdered BL collected in batch 2 is shown in Figure 2. The amorphous nature is evident by the hump centered approximately at 22° 2θ. According to the literature, the peaks at about 14° and 22° 2θ can be attributed to natural cellulose structures, as hemicellulose and lignin are amorphous.[39] Other peaks can be attributed to silicate polymorphs (mainly cristobalite) and to wollastonite (calcium silicate).

TGA suggested that the main mass losses due to thermal decomposition were completed at about 550°C (i.e., where the plateau in the derivative curve started, see Figure 3). A residual mass of about 32% was measured at 800°C, which is similar to the values reported in the literature.[36] Si extraction typically decreases with increasing combustion temperatures, due to the formation of more crystalline silicates in the ash, and it is suggested to keep combustion temperatures between 400 and 500°C.[24] On the other hand, the effects of impurities (i.e., other compounds such as $CaCO_3$) in the ash over the SS production is not clear. In order to explore some of these effects, the calcination of batch 1 was carried out at 550°C, whereas batches 2 and 3 were produced at 800°C. Two peaks in the derivative curve were observed at 283°C and 330°C, which were attributed to the pyrolysis of hemicellulose and cellulose respectively.[40]

3.1.2 | Bamboo leaves ash

After calcination, the ashes were collected and weighted. The ash content for calcination at 550°C (batch 1) was around 17%, whereas the calcination at 800°C (batches 2 and 3) led to an ash content equal to 11–12%. The chemical composition of BLA was assessed through SEM/EDS analysis on batch 1 and batch 3. Thirteen determinations on millimeter to sub-millimeter spots were carried out on four different SEM images of BLA from batch 1 (see Figure 4), whereas five EDS determinations on spots of about 250 × 250 μm were carried out on BLA from batch 3 (see Figure 5).

Table 4 summarises the average element contents and standard deviations assessed in SEM/EDS analysis. From the elemental analysis, it was possible to calculate the SiO_2 content of the ash from different batches. It was interesting to observe that the ash calcined at 550°C (batch 1) had a non-negligible content of C, which was considerably lower in batches calcined at 800°C. Despite a certain dispersion, results from the three batches lie in the same ranges. The SiO_2 content of BLA could be estimated at about 60%–65%.

Results from the XRF determination are shown in Table 5. However, the analysis of the data seemed to indicate contamination from iron and chromium (which were found disproportionately high), presumably from the steel tray used for the calcination of ash. The shape of metallic flakes was spotted on SEM images from batch 2 as well

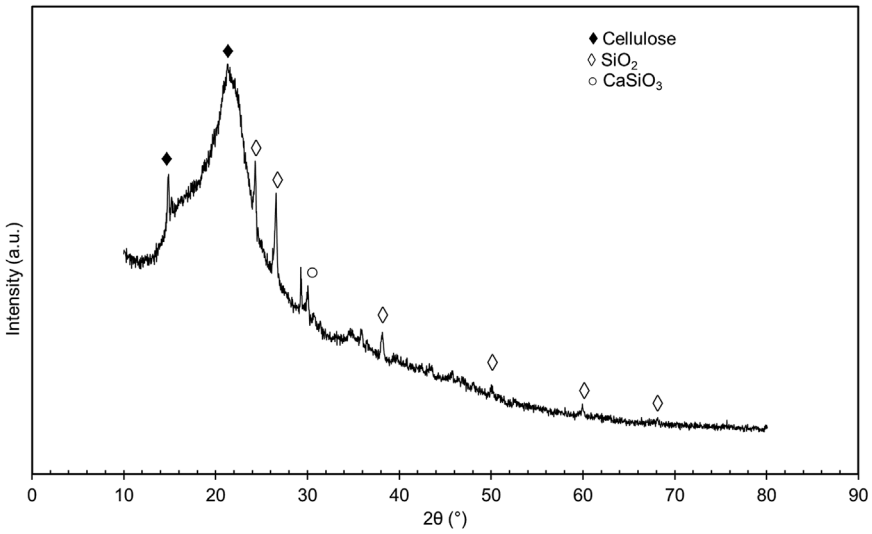

FIGURE 2 X-ray diffraction (XRD) diffractogram of bamboo leaves (batch 2) after oven drying at 70°C

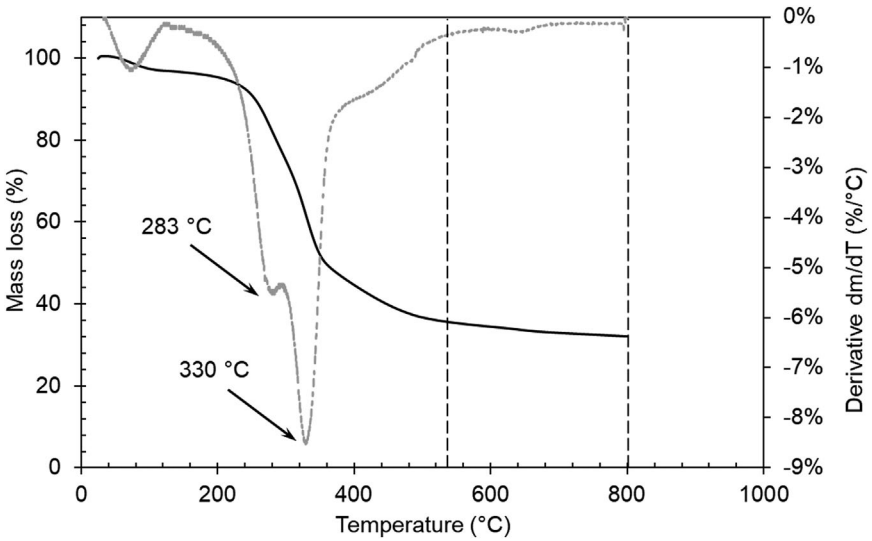

FIGURE 3 Thermo-gravimetric analysis (TGA)/DTG diagrams of bamboo leaves (BL) after oven drying at 70°C

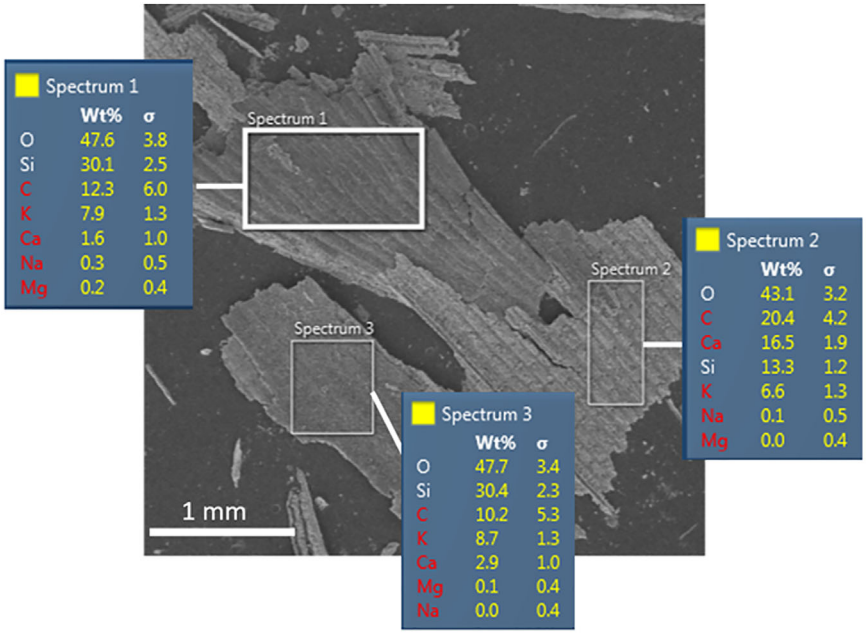

FIGURE 4 Example of scanning electron microscope coupled with energy-dispersive X-ray spectroscopy (SEM/EDS) analysis on BLA from batch 1

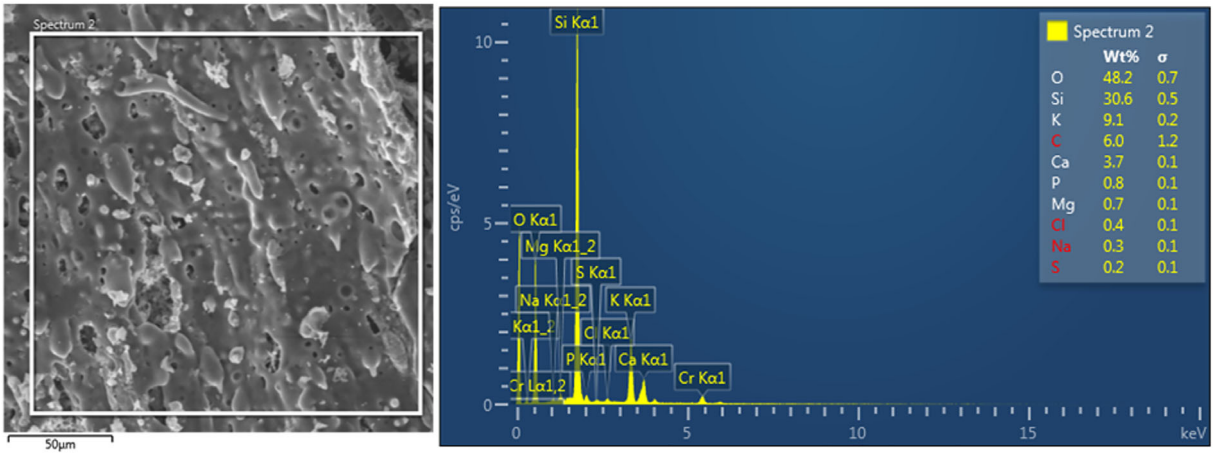

FIGURE 5 Example of scanning electron microscope coupled with energy-dispersive X-ray spectroscopy (SEM/EDS) analysis on BLA from batch 3

TABLE 4 Elemental composition of bamboo leaf ash (BLA) from scanning electron microscope coupled with energy-dispersive X-ray spectroscopy (SEM/EDS) analysis – main elements

Batch	O	Si	K	C	Ca	P	Mg	Calculated SiO_2
1	44.8 ± 3.2	21.5 ± 6.9	9.4 ± 1.8	14.4 ± 4.2	9.0 ± 7.2	–	–	46.1 ± 14.8
2*	43.1	30.4	7.3	–	5.2	1.0	0.9	65.0
3	51.0 ± 3.1	32.5 ± 3.6	8.0 ± 2.5	4.9 ± 1.0	2.9 ± 2.0	0.6 ± 0.2	0.6 ± 0.2	69.6 ± 7.8

*Data calculated from XRF analysis (see Table 5) after correction, see main text for details.

TABLE 5 Oxide composition from X-ray fluorescence (XRF) analysis for bamboo leaf ash (BLA) produced in batch 2

Oxide	SiO_2	K_2O	CaO	MgO	P_2O_5	Na_2O	Al_2O_3	MnO	Cr_2O_3	Fe_2O_3	Minor	LOI
1000°C	53.4	14.4	5.6	1.2	3.9	0.3	0.3	1.9	2.9	12.5	0.1	0.9
700°C	53.6	14.5	6.0	1.2	3.9	0.3	0.3	1.9	2.9	12.5	0.1	0.5

Abbreviation: LOI, loss on ignition.

as from batch 3. The SiO_2 amount from XRF analysis was used for the determination of NaOH dosage in the preparation of SS powder; however, this value might have been underestimated. By applying a correction (i.e., excluding Fe and Cr from the results and recalculating the composition of the ash) and calculating the elemental contents from the oxide contents for comparison purposes, data were close to those obtained with EDS for batches 1 and 3 (see Table 4), and SiO_2 content could have been assumed equal to 65%. However, this was not the case and in the calculations for the production of SS the value considered was 53%, as a conservative measure.

The XRD patterns of BLA from batches 1 and 3 are shown in Figure 6. A broad hump between 18 and 30° 2θ centered at 22° 2θ was observed in both samples, although more evident for BLA-1 (i.e., BLA from batch 1), confirming the amorphous nature of BLA. Diffraction peaks matching calcium carbonate were detected for BLA-1, as the furnace temperature was lower than the calcite decarbonation threshold, whereas these were not evident in BLA-3. Silicate polymorphs (quartz and cristobalite, with sharp peaks in BLA-3), sylvite, and potassium sulfate, as well as wollastonite traces, were also detected.

The presence of $CaCO_3$ in BLA-1 could explain its higher ash content (by about 5%) and the presence of C in the SEM/EDS analysis (see Table 4). The presence of sylvite and potassium sulfate is in agreement with the amount of K detected in the ashes and with the literature.

3.2 | Microstructure and mineralogical composition of BLA activator powder

Sodium silicate powder was produced according to the method suggested by Vinai and Soutsos[7] described in Section 2.2. The microstructural analysis of BLA-based

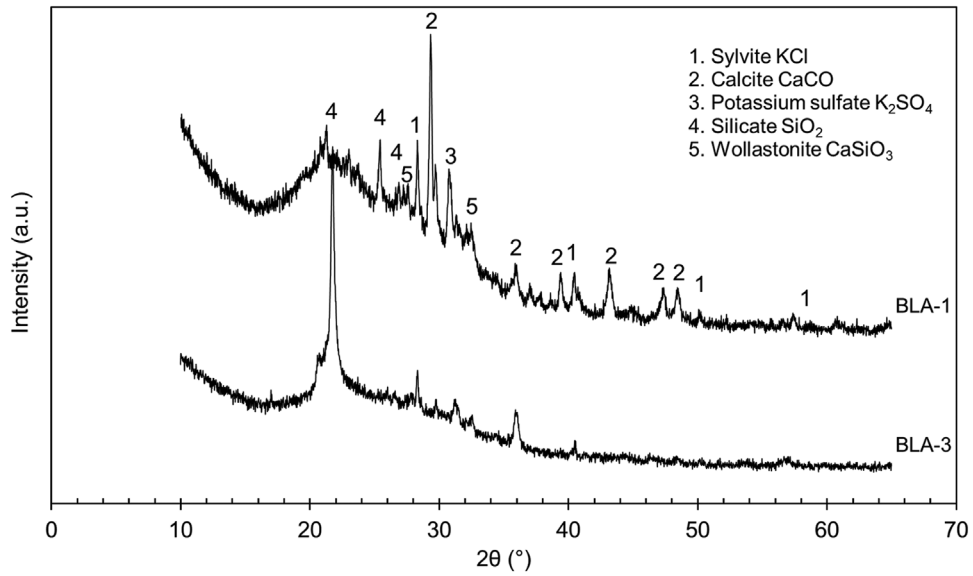

FIGURE 6 X-ray diffraction (XRD) diffractograms of BLA-1 (calcined at 550°C) and BLA-3 (calcined at 800°C)

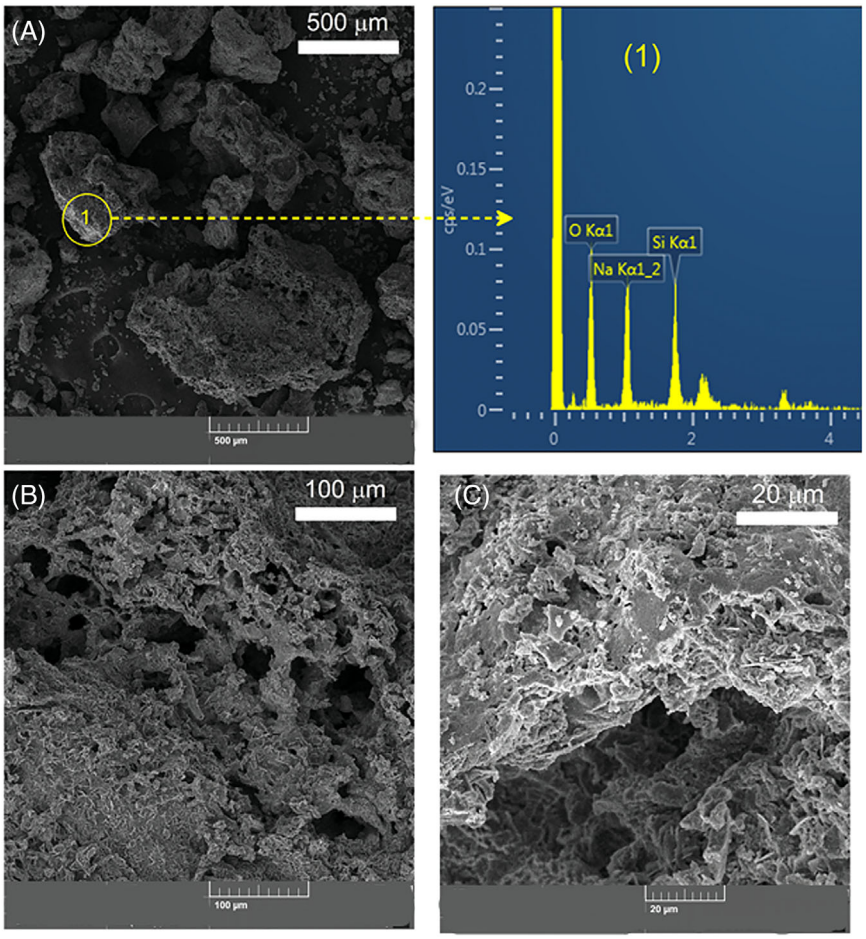

FIGURE 7 Scanning electron microscope coupled with energy-dispersive X-ray spectroscopy (SEM/EDS) analysis of sodium silicate activator powder: (A), (B), and (C) SEM of sodium silicate activator powder at 100x, 500x and 2.0kx Mag.[1] EDS analysis of spots 1, Na/Si = 1.157

SS (BLAA) powders was carried out with SEM-EDS tests to assess the effectiveness of reaction between BLA and NaOH, see Figure 7. The texture of reacted SS powder appears to be made of large round granules of a porous structure (Figure 7A). The pores were identified to be of a width of 20–50 μm (Figure 7B,C). The EDS analysis on the powder found a molar content of major elements with a Na/Si ratio in the range of 1.16–2.25.

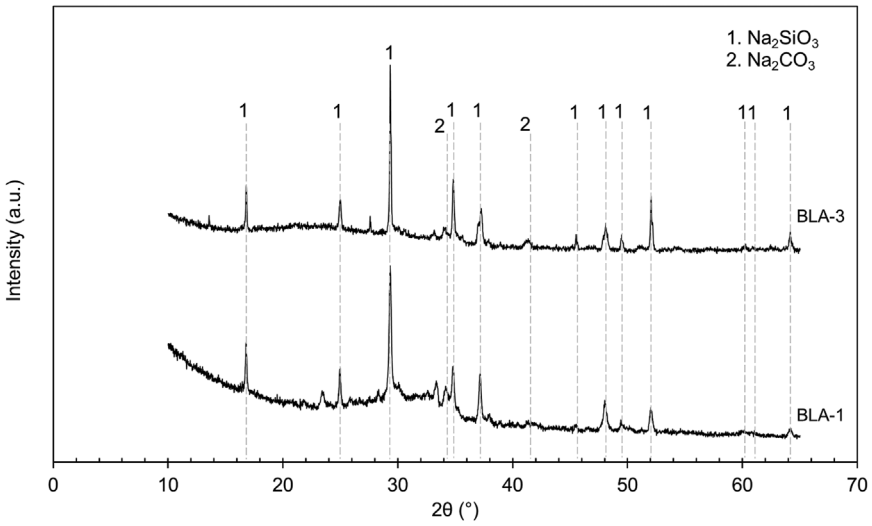

FIGURE 8 X-ray diffraction (XRD) diffractogram of sodium silicate activator powder

The mineralogical analysis of BLAA powder was further investigated using XRD to verify if peaks of crystalline SS could be found. The XRD diffractograms of the produced powders are shown in Figure 8, confirming the success of the thermochemical reaction that transformed the BLA into a crystalline powder with dominant peaks of Na_2SiO_3. Minor reflections from sodium carbonate were also detected. The shapes of the diffractograms seem to suggest that BLA-1 produced a less crystalline result, as presumably amorphous species not decomposed at 550°C were still present in the powder.

3.3 | Compressive strength of mortar cubes

The compressive strength of mortar cubes activated using BLAA was compared to that of control mortar samples activated with commercially available SS + NaOH (labeled SSSH) and mortar samples activated with NaOH only (labeled SH). Figure 9 summarises the results obtained from mortars produced with BLA from batch 1 tested at 1, 7, and 28 days of age (Figure 9A), as well as the comparison among mortar samples produced with different batches of BLA, tested at 7 days of age (Figure 9B). Results from batch 1 seem to suggest that BLA-based activator had slower reaction kinetics, as strengths at 1 day were very low, and values at 7 days of curing in standard indoor curing conditions were still lower than those of mortars activated with commercially available SS (Figure 9A). However, at 28 days the BLA-based mortar provided comparable strength, suggesting that the reaction was fully developed. The comparison between BLAA produced with the three batches of ash carried out analyzing the 7-day strength (see Figure 9B), suggested that the calcination temperature has a limited effect on the reactivity of the BLA for improving the strength development of the resulting binder in mortars.

Control samples manufactured with NaOH-only (samples SH) showed strengths significantly lower than those produced by including silicates in the activator, confirming that silicate species in BLAA were reactive and contributed to the strength development of the mortar.

The detrimental effect of an increase in w/s ratio on the compressive strength of AAM is well-documented in the literature. However, obtained results (Figure 9B) seem to suggest that compressive strengths of mixes were not significantly affected by the water content in the investigated range (i.e., w/s = 0.40–0.49). Results confirmed that BLAA can achieve strengths comparable with commercially available chemicals, and thus the ash-based SS powder is effective in its role of activator.

3.4 | Microstructure of pastes

Paste samples at 7 and 28 days of age were investigated with the SEM/EDS technique for observing the morphology of reacted material as well as determining the chemical composition of the binding matrix.

Figure 10 shows the morphology of the three samples at 7 days of age. It can be observed that in samples BLAA (see Figure 10A,B) there was a significant number of unreacted particles. FA particles are easily spotted as cenospheres in the matrix, whereas GGBS particles can be identified as lighter angular flakes. Nonetheless, the binding matrix has a fairly homogenous nature with glassy features (such as the crack edges that open on the surface), suggesting a good degree of reaction. When examining SSSH samples (see Figure 10C,D), a lower number of unreacted particles were observed, particularly in the image (D) where the surface is homogeneous and no cenospheres nor GGBS

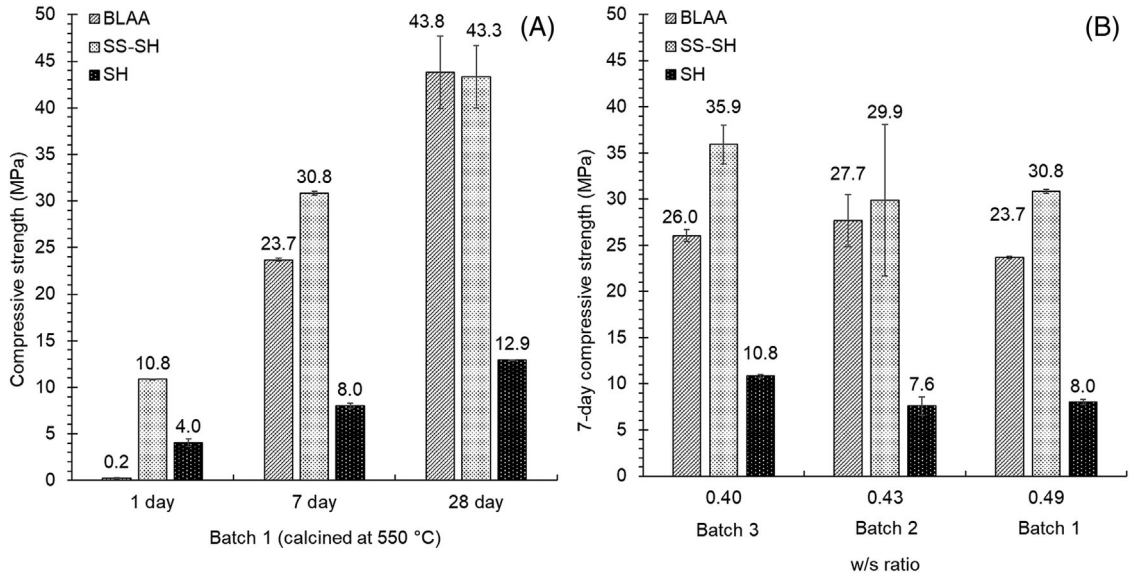

FIGURE 9 (A) Compressive strengths development over the time of the mortars (cured at room temperature ~20 C and 50% RH). (B) Comparison of 7-day compressive strength of mortars produced with different BLA batches for water to a solid ratio in the range 0.40–0.49

flakes can be spotted. The better dissolution of precursors can therefore explain the better mechanical properties of SSSH samples tested on mortars at 7 days compared to BLAA samples. However, the morphology of the matrix is not dissimilar to that of BLAA, suggesting the two materials have comparable nature. A significantly different morphology was instead observed in samples SH (see Figure 10E,F), where a large number of unreacted FA particles are surrounded by a binding matrix showing a globular appearance, significantly different from the glassy structure expected for AAM reaction products and found in the other mixes. The quality of the material suggests a poorly cemented gathering of particles, which would explain the significantly lower compressive strength recorded for SH samples.

The degree of dissolution of precursors can be appreciated from the EDS elemental mapping on Si, Al, Ca, and Na. Due to the chemical nature of precursors and activators, FA contributed with Si and Al, whereas GGBS provided Ca. Na was mainly provided by the activator. Figure 11 shows the comparison among the three samples. It can be observed that sample SSSH had a very homogeneous distribution of Si, Al, Ca, and Na, suggesting complete dissolution of the precursor and thorough incorporation of Na into the polymeric structure. Sample BLAA had a less homogeneous structure, with some of the unreacted particles still detected (such as anomalous concentrations of Si and Al in the same location, which suggests unreacted or partially reacted FA). Eventually, sample SH showed a very low level of dissolution, with most of the FA and GGBS particles still largely unreacted. The matrix around unreacted particles seems mainly composed of calcium species, suggesting that the SH activator was only able to dissolve Ca but could not trigger the complete release of Si and Al in the pore solution.

TABLE 6 Elemental analysis from energy-dispersive X-ray spectroscopy (EDS) on pastes at 28 days of curing

Sample	Si	Ca	Al	Ca/Si	Si/Al
BLAA	25.9±3.2	6.5±4.4	7.6±1.9	0.25	3.4
SSSH	27.5±4.1	7.1±0.4	7.5±0.9	0.26	3.7
SH	14.0±1.5	19.2±1.8	7.0±1.7	1.38	2.0

Abbreviations: BLAA, bamboo leaves ash-based activator; SH, sodium hydroxide; SSSH, commercially available sodium silicate + NaOH.

EDS analysis on points in the binding matrix at 28 days allowed to quantify the presence of Si, Al, and Ca in the reacted products. As discussed in Rafeet et al.,[41] the ratios of Ca/Si and Si/Al in the matrix can provide information over the nature of the binding gel. Table 6 summarizes the results of the EDS analysis. Three data points were collected on BLAA and SSSH samples, whereas two points were retained on the SH sample as one determination fell on the remnants of a FA cenosphere and thus were not considered representative of the reacted matrix.

It can be observed that the Ca/Si and Si/Al ratios for BLAA and SSSH samples were almost identical, confirming the substantially equivalent chemical nature of the reaction products in the two samples. Ca/Si ratios 0.2–0.6 suggest the formation of C-A-S-H type binding gel along with the geopolymer gel (N-A-S-H), which is expected for a FA/GGBS precursor blend having 40% GGBS. On the other hand, sample SH showed a significantly higher Ca/Si

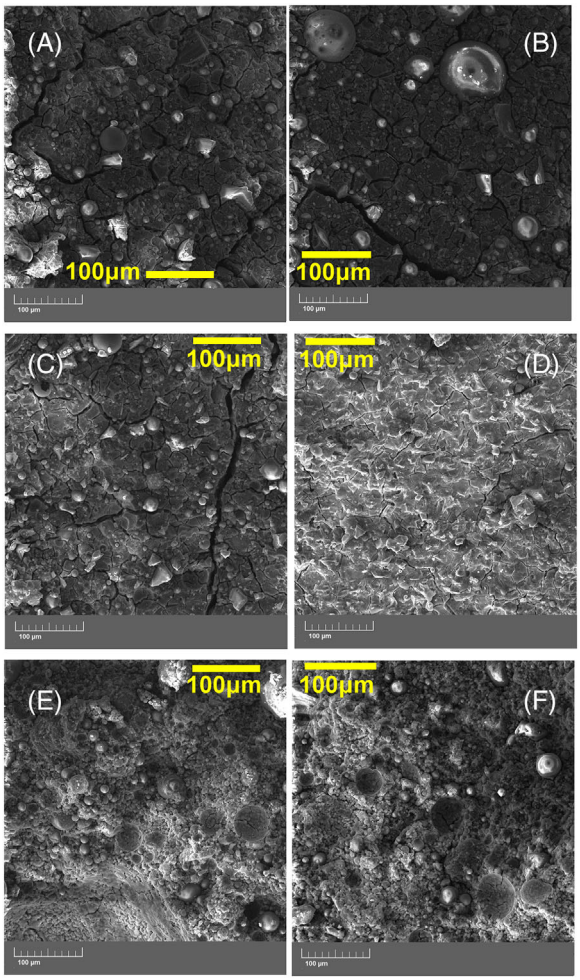

FIGURE 10 Scanning electron microscope (SEM) images of the pastes at 7 days. (A, B) bamboo leaves ash-based activator (BLAA), (C, D) commercially available sodium silicate + NaOH (SSSH), (E, F) sodium hydroxide (SH)

ratio, suggesting the dominance of Ca species in the matrix, and confirming that activation with neat NaOH produced mainly the hydration of Ca species in GGBS rather than triggering the Si-Al polymeric structure that would be expected in AAM. The Ca/Si ratio equal to 1.38 is higher than those reported in the literature (i.e., in the range of 1.0–1.2) for alkali-activated slag systems, and is more similar to that found in C-S-H gel in Portland cement (in the range of 1.2–2.3).[41]

3.5 | Environmental implications

The investigation aimed at understanding the potential for BLA to be transformed in SS for the activation of AAM by applying the low-cost and low-energy thermochemical method proposed by Vinai and Soutsos.[7] It was observed that ash obtained either at 500 or 800°C was suitable for the production of SS powder. This aspect is very important in the perspective of co-production of ash from biomass-fuelled power stations in emerging economy countries, where most of the bamboo is currently produced, and therefore the availability of leaves as a by-product of the harvest is higher. As demonstrated by Moraes et al.,[42] the BLA obtained by auto-combustion process had a high content of SiO_2 (74%) in amorphous form, as well as satisfactory pozzolanicity and reactivity.

The environmental investigation carried out using life cycle assessment tools by Bianco et al.[9] suggested that alkali-activated concrete produced with waste glass-based activator obtained through the same thermochemical method adopted in this study resulted in carbon emissions of about 100–120 $kgCO_{2eq}/m^3$ for concretes having compressive strength in the range 35–50 MPa. In the same study, CO_2 emissions of Portland cement-based concretes were calculated in the range 333 to 409 $kgCO_{2eq}/m^3$ for equivalent strength classes. The study highlighted that the grinding of glass had a marginal impact on the emissions of the waste-derived activator, and about 67–69 kg of activating powder was required for about 355–370 kg of the binder.[7,9]

The mix proportions shown in Table 2 (see Section 2.2) were in the same order of magnitude (about 100 g of powder for 500 g of binder, which corresponds to 72 kg of powder for 360 kg of binder), and the compressive strength of mortars was in the range of 40 MPa at 28 days. Since the process for producing the activating powder is the same, the activator dosages are comparable, and the strength is in the same range, it can be assumed that the CO_2 emissions of concrete produced with BL-based activating powder could be in the range 100–120 $kgCO_{2eq}/m^3$. This value does not consider the CO_2 emitted during the combustion of BL. For this latter, an estimate can be carried out assuming that:

- The carbon content of bamboo foliage is about 41.5% of dry matter.[43]
- The ash content is about 12% (this study)
- The ratio ash/activating powder is 0.60 (this study).

Under these assumptions, about 362 kg of BL would be required for producing 72 kg of ash, corresponding to about 150 kg of C, which would react with O_2 during combustion emitting about 550 kg of CO_2. However, the allocation of this CO_2 mass is not straightforward, because:

- Under the assumption that the ash is obtained from a BL biomass-fuelled power plant, the ash is a by-product, and thus should be considered burden-free. Obviously,

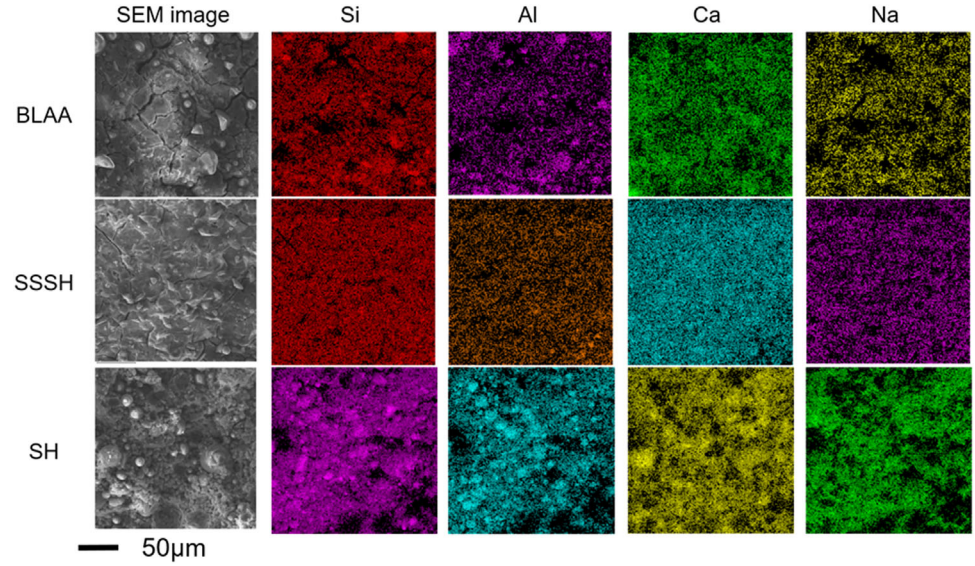

FIGURE 11 Scanning electron microscope coupled with energy-dispersive X-ray spectroscopy (SEM/EDS) elemental mapping of the pastes at 7 days

the combustion of leaves exclusively for obtaining the ash is not an option.

- Due to the exceptional growth rate of bamboo, the emitted CO_2 could be assumed to be sequestrated again by the next generation of bamboo plants in a short time,[43] and thus a closed carbon loop model could be adopted.

Bamboo sequestrates CO_2 in the foliage and culm as well as in the ground, and thus a complete analysis of the CO_2 emission versus sequestration should be carried out for the assessment of the net impact/benefit. A holistic analysis of the possible overall environmental impact of an entire value chain consisting of construction element (bamboo culm vs. timber) + energy production (combustion of BL vs. fossil fuels) + concrete production (AAM concrete vs. Portland cement-based concrete) could look promising when compared to the existing value chain.

4 | CONCLUSIONS

This paper presents an investigation of the production of a bio-based SS powder from BLA. This study confirms the use of BMA as an alternative silica source for low cost and potentially low carbon footprint powder activator for alkali-activated concrete. From the outcomes of this study, it can be concluded that:

- BLA is a suitable silica source for the development of an SS powdered activator. The production process involves the combination of BLA, SH pellets, and water, heated in an oven at 300°C for 1 h.
- The efficiency of the developed powder was investigated through the analysis of XRD diffractograms of the obtained powder. The investigation confirmed the crystalline nature of the powder with SS species of various SiO_2/Na_2O molar ratios.
- The strength development at 1, 7, and 28 days of mortars produced with BLA-based activator was compared against that of samples manufactured with commercially available SS and SH solutions. Although strength at 1 day was lower than the benchmark, strength values of about 25 MPa were recorded at 7 days, irrespective of the water/solid ratio in the mix and the calcination temperature of BL. Strength at 28 days matched the benchmark, exceeding 40 MPa.
- Microstructural analysis confirmed that the lower strength of BLA-based mortars at 7 days could be due to the non-complete dissolution of precursors in the matrix. The morphology and the elemental mapping (Si, Al, Ca, and Na) from EDS analysis showed that the silicates in BLAA were effective in producing a better quality binding matrix when compared to neat SH –activated samples.
- The Ca/Si ratio and Si/Al ratio confirmed that the nature of calcium-aluminum-silicate-hydrate gel (CASH) in pastes manufactured with BLAA and commercial chemicals was similar.

The extension of the method to other BMAs will allow us to determine the impact of ash composition variability on the performance of the activator powder. Furthermore, the use of ash from industrial boilers will provide insights into the suitability of combustion by-products

from biomass-fuelled power generation in the production of SS for AAM manufacture.

ACKNOWLEDGMENTS

The support of Dr. Hong Chang (University of Exeter) in SEM/EDS analysis is gratefully acknowledged. The research data supporting this publication are provided within this paper.

AUTHOR CONTRIBUTIONS

Raffaele Vinai: conceptualization, supervision, data analysis, writing, and approval. Fabrice Ntimugura: data analysis and writing. Will Cutbill: experimentation and data collection. Robert Evans: experimentation and data collection. Yize Zhao: experimentation and data collection.

REFERENCES

1. Costa F, Ribeiro D. Reduction in CO_2 emissions during production of cement, with partial replacement of traditional raw materials by civil construction waste (CCW). J Clean Prod. 2020;276:123302.
2. McLellan BC, Williams RP, Lay J, van Riessen A, Corder GD. Costs and carbon emissions for geopolymer pastes in comparison to ordinary portland cement. J Clean Prod. 2011;19(9-10):1080–90.
3. Jamieson E, McLellan B, Van Riessen A, Nikraz H. Comparison of embodied energies of ordinary portland cement with bayer-derived geopolymer products. J Clean Prod. 2015;99:112–8.
4. Habert G, de Lacaillerie JBD, Roussel N. An environmental evaluation of geopolymer based concrete production: reviewing current research trends. J Clean Prod. 2011;19(11):1229–38.
5. Passuello A, Rodriguez ED, Hirt E, Longhi M, Bernal SA, Provis JL, et al. Evaluation of the potential improvement in the environmental footprint of geopolymers using waste-derived activators. J Clean Prod. 2017;166:680–9.
6. Tong KT, Vinai R, Soutsos MN. Use of Vietnamese rice husk ash for the production of sodium silicate as the activator for alkali-activated binders. J Clean Prod. 2018;201:272–86.
7. Vinai R, Soutsos M. Production of sodium silicate powder from waste glass cullet for alkali activation of alternative binders. Cement Concrete Res. 2019;116:45–56.
8. Abdulkareem M, Havukainen J, Nuortila-Jokinen J, Horttanainen M. Environmental and economic perspective of waste-derived activators on alkali-activated mortars. J Clean Prod. 2020:124651.
9. Bianco I, Tomos BAD, Vinai R. Analysis of the environmental impacts of alkali-activated concrete produced with waste glass-derived silicate activator–a LCA study. J Clean Prod. 2021;316:128383.
10. Samarakoon M, Ranjith P, Duan WH, De Silva V. Properties of one-part fly ash/slag-based binders activated by thermally-treated waste glass/NaOH blends: a comparative study. Cem Concr Compos. 2020:103679.
11. Alnahhal MF, Kim T, Hajimohammadi A. Waste-derived activators for alkali-activated materials: a review. Cem Concr Compos. 2021:103980.
12. Figueiredo RA, Brandão PR, Soutsos M, Henriques AB, Fourie A, Mazzinghy DB. Producing sodium silicate powder from iron ore tailings for use as an activator in one-part geopolymer binders. Mater Lett. 2021;288:129333.
13. Puertas F, Torres-Carrasco M. Use of glass waste as an activator in the preparation of alkali-activated slag. Mechanical strength and paste characterisation. Cement Concrete Res. 2014;57:95–104.
14. Bernal SA, Rodríguez ED, de Gutiérrez RM, Provis JL, Delvasto S. Activation of metakaolin/slag blends using alkaline solutions based on chemically modified silica fume and rice husk ash. Waste Biomass Valorization. 2012;3(1):99–108.
15. Billong N, Oti J, Kinuthia J. Using silica fume based activator in sustainable geopolymer binder for building application. Constr Build Mater. 2021;275:122177.
16. Vassilev SV, Baxter D, Andersen LK, Vassileva CG. An overview of the composition and application of biomass ash. Part 1. Phase–mineral and chemical composition and classification. Fuel 2013;105:40–76.
17. Imbabi MS, Carrigan C, McKenna S. Trends and developments in green cement and concrete technology. Int J Sustain Built Environ. 2012;1(2):194–216.
18. Martirena F, Monzó J. Vegetable ashes as supplementary cementitious materials. Cement Concrete Res. 2018;114:57–64.
19. Aprianti E, Shafigh P, Bahri S, Farahani JN. Supplementary cementitious materials origin from agricultural wastes–a review. Constr Build Mater. 2015;74:176–87.
20. Matalkah F, Soroushian P, Abideen SU, Peyvandi A. Use of non-wood biomass combustion ash in development of alkali-activated concrete. Constr Build Mater. 2016;121:491-500.
21. Abdulkareem OA, Ramli M, Matthews JC. Production of geopolymer mortar system containing high calcium biomass wood ash as a partial substitution to fly ash: An early age evaluation. Composites Part B. 2019;174:106941.
22. Yusuf MO, Johari MAM, Ahmad ZA, Maslehuddin M. Evolution of alkaline activated ground blast furnace slag–ultrafine palm oil fuel ash based concrete. Mater Design. 2014;55:387–93.
23. Moraes J, Font A, Soriano L, Akasaki J, Tashima M, Monzó J, et al. New use of sugar cane straw ash in alkali-activated materials: a silica source for the preparation of the alkaline activator. Constr Build Mater. 2018;171:611–21.
24. Dodson JR, Hunt AJ, Budarin VL, Matharu AS, Clark JH. The chemical value of wheat straw combustion residues. RSC Adv. 2011;1(3):523–30.
25. Dodson J, Cooper E, Hunt A, Matharu A, Cole J, Minihan A, et al. Alkali silicates and structured mesoporous silicas from biomass power station wastes: the emergence of bio-MCMs. Green Chem. 2013;15(5):1203–10.
26. Goh Y, Yap SP, Tong TY. Bamboo: the emerging renewable material for sustainable construction. In: Hashmi S, editor. Reference module in materials science and materials engineering. Amsterdam:. Elsevier; 2019. p. 1–14.
27. De Flander K, Rovers R. One laminated bamboo-frame house per hectare per year. Constr Build Mater. 2009;23(1):210–8.
28. Gratani L, Crescente MF, Varone L, Fabrini G, Digiulio E. Growth pattern and photosynthetic activity of different bamboo species growing in the Botanical Garden of Rome. Flora - Morphol Distrib Funct Ecol Plants. 2008;203(1):77–84.

29. Shanmughavel P, Francis K. Above ground biomass production and nutrient distribution in growing bamboo (Bambusa bambos (L.) Voss). Biomass Bioenergy. 1996;10(5–6):383–91.
30. Numata M, Ikusima I, Ohga N. Ecological aspects of bamboo flowering ecological studies of bamboo forests in Japan, XIII. J Plant Res. 1974;87(4):271–84.
31. Shanmugam M, Sivakumar G, Arunkumar A, Rajaraman D, Indhira M. Fabrication and assessment of reinforced ceramic electrical insulator from bamboo leaf ash waste. J Alloys Compd. 2020;824:153703.
32. Dwivedi V, Singh N, Das S, Singh N. A new pozzolanic material for cement industry: bamboo leaf ash. Int J Phys Sci. 2006;1(3):106–11.
33. Villar-Cociña E, Morales EV, Santos SF, Savastano H Jr, Frías M. Pozzolanic behavior of bamboo leaf ash: characterization and determination of the kinetic parameters. Cem Concr Compos. 2011;33(1):68–73.
34. Frías M, Savastano H, Villar E, de Rojas MIS, Santos S. Characterization and properties of blended cement matrices containing activated bamboo leaf wastes. Cem Concr Compos. 2012;34(9):1019–23.
35. Kolawole JT, Olusola KO, Babafemi AJ, Olalusi OB, Fanijo E. Blended cement binders containing bamboo leaf ash and ground clay brick waste for sustainable concrete. Materialia 2021;15:101045.
36. Kow K-W, Yusoff R, Aziz AA, Abdullah E. From bamboo leaf to aerogel: preparation of water glass as a precursor. J Non Cryst Solids. 2014;386:76–84.
37. Olawale O, Akinyemi B, Ogundipe S, Abayomi S, Adekunle A. Response surface methodology for silicon production from bamboo leaves. IOP Conf Ser Earth Environ Sci. 2021;65(1):012075.
38. Luukkonen T, Abdollahnejad Z, Yliniemi J, Kinnunen P, Illikainen M. One-part alkali-activated materials: a review. Cement Concrete Res. 2018;103:21–34.
39. Yueping W, Ge W, Haitao C, Genlin T, Zheng L, Feng XQ, et al. Structures of bamboo fiber for textiles. Text Res J. 2010;80(4):334–43.
40. Fan B, Yao Q, Wang C, Jin C, Wang H, Xiong Y, et al. Natural cellulose nanofiber extracted from cell wall of bamboo leaf and its derived multifunctional aerogel. Polym Compos. 2018;39(11):3869–76.
41. Rafeet A, Vinai R, Soutsos M, Sha W. Effects of slag substitution on physical and mechanical properties of fly ash-based alkali activated binders (AABs). Cement Concrete Res. 2019;122:118–35.
42. Moraes M, Moraes J, Tashima M, Akasaki J, Soriano L, Borrachero M, et al. Production of bamboo leaf ash by autocombustion for pozzolanic and sustainable use in cementitious matrices. Constr Build Mater. 2019;208:369–80.
43. Amoah M, Assan F, Dadzie PK. Aboveground biomass, carbon storage and fuel values of Bambusa vulgaris, Oxynanteria abbyssinica and Bambusa vulgaris var. vitata plantations in the Bobiri forest reserve of Ghana. J Sustain For. 2020;39(2):113–36.
44. Huseien GF, Hamzah HK, Sam AR, Khalid NH, Shah KW, Deogrescu DP, et al. Alkali-activated mortars blended with glass bottle waste nano powder: Environmental benefit and sustainability. J Cleaner Prod. 2020;243:118636.
45. Novoselova LY. Hematite nanopowder obtained from waste: Iron-removal sludge. Powder Technol. 2016;287:364–72.
46. Stalin S, Edukondalu A, Boukhris I, Alrowaili ZA, Al-Baradi AM, Olarinoye IO, et al. Effects of TeO_2/B_2O_3 substitution on synthesis, physical, optical and radiation shielding properties of $ZnO–Li_2O\text{-}GeO_2\text{-}Bi_2O_3$ glasses. Ceram Int. 2021;47(21):30137–46.

How to cite this article: Vinai R, Ntimugura F, Cutbill W, Evans R, Zhao Y. Bio-derived sodium silicate for the manufacture of alkali-activated binders: Use of bamboo leaf ash as silicate source. Int J Appl Ceram Technol. 2022; 1–14. https://doi.org/10.1111/ijac.14004